Estimating Surface Reflectance and Albedo from Landsat-5 Thematic Mapper over Rugged Terrain

Claude R. Duguay
Laboratory for Earth Observation and Information Systems, Department of Geography, University of Ottawa, Ottawa, Ontario K1N 6N5, Canada
Ellsworth F. LeDrew
Earth-Observations Laboratory, Institute for Space and Terrestrial Science and Department of Geography, University of Waterloo, Waterloo, Ontario N2L 3G1, Canada

ABSTRACT: A model for estimating surface reflectance and albedo from satellite radiance measurements over rugged terrain is presented. Using a two-stream radiative transfer model, direct and diffuse sky irradiance as well as path radiance and atmospheric transmission are calculated for a horizontally homogeneous atmosphere. A digital elevation model is used to estimate these parameters for surfaces of varying elevation, slope, and aspect. The satellite- derived, corrected reflectance measurements obtained from Landsat Thematic Mapper Bands 2, 4, and 7 are integrated into a measure of albedo by the use of a weighted average scheme which takes into account the spectral reflectivity of the surface of interest as well as the spectral distribution of total shortwave irradiance. The model is then tested over an area in the east slope of the Colorado Front Range. Estimated values of albedo for selected surfaces in the alpine tundra are in substantial agreement with published data for comparable surfaces and field measurements in the region.

INTRODUCTION

SURFACE ALBEDO IS USED IN CLIMATE MODELS to specify the amount of solar radiation absorbed at the surface. Information regarding the spatial and temporal variability of surface albedo is thus important in climate studies from the local to the global scale. Earth-sensing satellites, such as Landsat, have the potential to provide albedo measurements at the scale of drainage basins (Dozier, 1989). At this scale, surface albedo measurements are of particular interest in studies of ecosystem dynamics, hydrology, and geomorphology of alpine environments.

However, several factors complicate the estimation of surface albedo from remotely sensed data: (1) the atmospheric effects, (2) the degree of isotropy of the surface being sensed and, (3) the spectral interval of the narrow band sensor (Brest and Goward, 1987). In rugged terrain, the geometry between the sun, the surface orientation, and the satellite sensor, which can vary from one pixel to another, is an additional factor which makes the estimation of surface reflectance from remotely sensed data difficult (Proy *et al.*, 1989).

Recent studies have shown the complexity of deriving the reflection characteristics of the Earth surface from satellite sensors over mountainous terrain (Woodham and Gray, 1987; Dozier, 1989; Proy *et al.*, 1989; Yang and Vidal, 1990). In these studies, attempts have generally been made to gain a better understanding of the various possible sources of solar radiation in alpine areas as well as improving their estimates. The computation of terrain-reflected irradiance (i.e., the portion of incoming radiation which is reflected by adjacent terrain), however, remains a major obstacle to more precise estimates of surface reflectance. This parameter is difficult and time expensive to compute because it requires information on the spectral albedo of the ground cover, which is usually not known *a priori*, the orientation of the terrain with respect to a close topographic set, and the exposure of the slope. In order to overcome this problem, Proy *et al.* (1989) recommended that one work with satellite images acquired at high solar elevation angles (greater than 45°). They have shown that the terrain-reflected irradiance can be neglected in the derivation of reflectance for well-illuminated surfaces, but cannot be ignored for shadowed surfaces (e.g., deep valleys).

Another issue of concern, but which has received little attention, is the quality of digital elevation models (DEMs). Although frequently used in conjunction with remotely sensed imagery for improving land-cover classifications or determining the reflectance characteristics of surfaces in mountainous terrain, uncertainties associated with the quality of DEMs are often ignored. In a recent article on the spectral signature of alpine snow cover using TM imagery, Dozier (1989) indicates that "... the (his) detailed model of interaction between radiation and the terrain can only be used for simulation, because the quality of most digital elevation data is not good enough to calculate the slope and aspect of each pixel. Errors in the original elevation data are magnified by the differencing operations needed to compute the local gradient." The question related to the quality of DEMs is addressed herein.

In this study, we describe a model for estimating surface reflectance and albedo over rugged terrain using Landsat-5 TM imagery. Using a two-stream radiative transfer model, remotely sensed observations are used in combination with a digital elevation model and radiosonde measurements to derive surface reflectance. The visible, near-infrared, and mid-infrared reflectance derived from Landsat TM spectral bands 2, 4, and 7 are combined into a measure of albedo by the use of weighted average formulae, similar in a sense to the one described by Brest and Goward (1987) using Landsat MSS data. Estimated values of surface reflectance and albedo for selected surfaces are compared to published data for comparable surfaces and ground based measurements acquired during two field seasons over an alpine tundra site in the Colorado Front Range. The quality of an albedo map produced following the proposed procedure is then evaluated.

DESCRIPTION OF THE MODEL

DERIVATION OF SURFACE REFLECTANCE

The term surface reflectance, as used herein, is defined as the ratio of energy reflected by a surface under specified con-

PHOTOGRAMMETRIC ENGINEERING & REMOTE SENSING,
Vol. 58, No. 5, May 1992, pp. 551–558.

0099-1112/92/5805-551$03.00/0

ditions of illumination and viewing to that reflected by a Lambertian surface, identically illuminated and viewed (Woodham and Gray, 1987; Yang and Vidal, 1990). It is a measurable descriptive of the reflection characteristics of the surface and invariant to the atmosphere or topography. Surface reflectance is also understood to be specifically limited to a narrow waveband or single wavelength. Surface albedo, on the other hand, is used as a substitute for the integrated hemispherical albedo, from three narrow bands of Landsat TM data (TM2, TM4, and TM7) from which it is derived (Brest and Goward, 1987). Albedo is defined as the ratio of the radiation reflected by a surface to the radiation incident upon it. Its measurement implies integration over the complete sphere of all directions and wavelengths (e.g., 0.28 to 6.00 μm).

With our current state of knowledge about the radiative transfer to a spherical Earth, the determination of surface reflectance from remotely sensed data requires a number of simplifying assumptions; a full treatment of all components of the scene radiance equation is currently not feasible (Woodham and Lee, 1985; Yang and Vidal, 1990). In our model, the sensor is assumed to view the surface from directly overhead and the ground cover is assumed to be Lambertian with bidirectional reflectance distribution function (BRDF) $f_r = \rho / \pi$, where ρ is the surface reflectance.

Surface reflectance for each TM reflective band is calculated as

$$\rho[i] = \pi (L[i] - L_p[i,z]) / (T_v[i,z] E[i,z]) \quad (1)$$

where $L[i]$ is the sensor radiance for a given TM band $[i]$ associated with the surface, $L_p[i,z]$ is the path radiance between the sensor and the surface at altitude z, $T_v[i,z]$ is the vertical transmission from altitude z up to the sensor, and $E[i,z]$ is the total solar irradiance on an inclined surface at altitude z. In the calculation of reflectance, all components computed from the radiative transfer model are integrated over the bandwidth of interest so that $L[i]$ and $L_p[i,z]$ are expressed in Wm^{-2} sr^{-1} and $E[i]$ in Wm^{-2}.

Sensor radiance

The sensor radiance is calculated as

$$L[i] = A_0[i] + A_1[i]DC[i] \quad (2)$$

where $A_0[i]$ and $A_1[i]$ are the calibration coefficients associated with a given TM band and DC is the digital count. The values of the calibration coefficients are available from the header files of the TM images (Table 1).

Solar irradiance

The total in-band (i) solar irradiance for a given surface at altitude z can be computed as follows:

$$E[i,z] = \phi E_{Sh}[i,z] (\cos I/\cos I_h) + E_{Dh}[i,z] \{K'[i,z] (\cos I/\cos I_h) + 0.5 (1 - K'[i,z]) (1 + \cos s)\} + 0.5 \alpha E_h[i,z] (1 - \cos s) \quad (3)$$

where

TABLE 1. LANDSAT-5 TM RADIANCE CONVERSION PARAMETERS

Band	Wavelength (μm)	Gain (A_1) (Wm^{-2} sr^{-1} μm^{-1} DC^{-1})	Offset (A_0) (Wm^{-2} sr^{-1} μm^{-1})
TM1	0.45-0.52	0.0602	−0.1500
TM2	0.52-0.60	0.1175	−0.2805
TM3	0.63-0.69	0.0806	−0.1194
TM4	0.76-0.90	0.0814	−0.1500
TM5	1.55-1.75	0.0108	−0.0370
TM7	2.08-2.35	0.0057	−0.0150

ϕ = a binary coefficient, and is set to zero whenever a surface is shadowed by surrounding ridges (cast shadow) or faces away from the sun (self-shadow),

$E_h[i,z]$ = total solar irradiance to an unobstructed horizontal surface,

$E_{Dh}[i,z]$ = diffuse sky irradiance to an unobstructed horizontal surface,

$E_{Sh}[i,z]$ = direct solar irradiance to an unobstructed horizontal surface,

I = the angle of incidence of direct irradiance,

I_h = the angle of incidence of direct irradiance referenced to an unobstructed horizontal surface,

$K'[i,z]$ = anisotropy index used to separate diffuse sky irradiance into isotropic and circumsolar components, and

s = the slope of the surface in question.

The direct, diffuse sky, and total solar irradiance to unobstructed horizontal surfaces can either be estimated from two-radiative transfer calculations, such as PIFM (Zdunkowski *et al.*, 1982) or LOWTRAN 7 (Kneizys *et al.*, 1988), or acquired during field measurement campaigns. These parameters can then be combined with a digital elevation model in order to calculate incoming radiative fluxes for all elevations within a given study area. For the reasons indicated earlier in this paper, the last portion of the equation ($0.5 \alpha E_h[i,z] (1 - \cos s)$), which represents the contribution of terrain-reflected radiation, is not computed at the present time in our model.

I_h is simply computed as the cosine of the solar zenith angle. The anisotropy index K' is the ratio of the direct solar irradiance on a surface normal to the sun to that of the solar irradiance on that same surface at the top of the atmosphere (Hay, 1983). Recent studies have indicated that a proper treatment of the anisotropy of diffuse sky illumination can improve irradiance estimates (Cavayas *et al.*, 1983; Teillet, 1986; Proy *et al.*, 1989). The angle of incidence of direct irradiance is computed using the following equation (Robinson, 1966):

$$I = \cos^{-1} (\cos(s) \cos(Z_s) + \sin(s) \sin(Z_s) \cos(A_s - A_z)) \quad (4)$$

where s and A_s are the slope and aspect of the surface, derived from a digital elevation model, and Z_s and A_z the solar zenith and azimuth angles.

Vertical transmission and path radiance

The vertical atmospheric transmission attenuates the surface radiance of a point at altitude z reaching the sensor. This term can be evaluated if total irradiance on an unobstructed horizontal surface, as well as the extraterrestrial solar flux density to a horizontal surface, are known. The atmospheric transmission within a spectral band can be determined as the ratio between total in-band shortwave irradiance on a horizontal surface (E_h) and extraterrestrial solar irradiance (E_0) (Liu and Jordan, 1960; Olyphant, 1984). It is given by

$$T_v[i,z] = E_h[i,z] / E_0[i]. \quad (5)$$

The atmospheric transmission varies exponentially as a function of terrain height [z] such that there is an increase in transmission with an increase in elevation (Woodham and Lee, 1985). According to Sjoberg and Horn (1983), this is a reasonable assumption under clear sky conditions when Mie scattering is minimized.

Path radiance is the energy that reaches the sensor due to backscatter from the direct solar beam, including both single and multiple scattering. Single scattering from the direct solar beam, called primary scattering, is the major component of path radiance in optically thin atmospheres. The adjacency effect is

small in areas of low reflectance but may become significant as the reflectance of the ground increases. In mountainous terrain, path radiance has also been shown to vary exponentially as a function of altitude (Sjoberg and Horn, 1983).

When acceptable calibration targets are not available (e.g. clear lakes or shadowed areas), the effects due to primary scattering can be calculated from a two-stream radiative transfer model by assigning a surface albedo of zero to the lowest target point in the study area. All energy radiating from the surface to the sensor can thus be considered as path radiance. The second source of path radiance has been shown to be negligible under clear skies (Woodham and Gray, 1987).

Derivation of Surface Albedo

An accurate measure of albedo from remotely sensed reflectance measurements can be derived when the following three factors are considered (Brest and Goward, 1987): (1) the spectral reflectance of the surface of interest; (2) the spectral distribution of the irradiance; and (3) the wavelength region of the discrete spectral bands. In our model, the spectral distribution of solar irradiance is considered to be within the 0.28- to 6.00-fm range.

The determination of albedo from reflectance measurements requires that the spectral reflectance curve of the object being sensed be divided into segments of uniform reflectance. Each segment of the curve can then be represented by a band measurement located within the range of the segment. The procedure proposed by Brest and Goward (1987) and Brest (1987) for MSS data is adapted to Landsat TM herein. An advantage of using TM over MSS is that we have the possibility to use a mid-infrared band (TM5 or TM7) for the estimation of surface albedo. In this approach, a weighting scheme is assigned to a particular category based on the spectral reflectance curve characterizing it. Different weighting schemes are used to derive albedo from reflectance measurements for vegetated, non-vegetated (water, bare soil, rock, etc.), and snow covered surfaces.

Vegetated surfaces

Vegetated surfaces have three distinct segments of reflectance. These can be characterized as low reflectance in the visible, high reflectance in the near infrared, and medium to low reflectance in the mid infrared. The weighting scheme used for the determination of surface albedo of vegetation from TM reflectance measurements is then:

$$\alpha = 0.526\ (\rho[\text{TM2}]) + 0.362\ (p[\text{TM4}]) + 0.112\ (\rho[\text{TM7}]). \quad (8)$$

In this equation, 0.526, 0.362, and 0.112 represent the proportional weighting factors for the visible, near-infrared, and mid-infrared portions of the spectrum, respectively. These factors simply account for the portion of the total solar irradiance (0.28 to 6.00 fm) within the three segments.

Non-vegetated surfaces

Non-vegetated surfaces, with the exception of snow, have less complicated spectral curves. Thus, a two part weighting scheme is used to estimate albedo for non-vegetated surfaces. Here, the EM spectrum is subdivided into two regions: a visible and an infrared region. The visible segment has its lower and upper limits at 0.28 and 0.725 fm, respectively, and the infrared segment is situated between 0.725 and 6.00 fm. The proportional weighting factors are 0.526 for the visible and 0.474 for the infrared. The albedo for non-vegetated surfaces is thus estimated as

$$\alpha = 0.526\ (\rho[\text{TM2}]) + 0.474\ (\rho[\text{TM4}]). \quad (9)$$

Snow covered surfaces

Two weighting schemes were derived for snow covered surfaces by partitioning the reflectance curve into four regions: 0.28 to 0.725, 0.725 to 1.00, 1.00 to 1.40, and 1.40 to 6.00 μm. Snow reflectance is very high in the visible portion of the electromagnetic spectrum, but decreases rapidly in the near infrared and mid infrared wavelengths. In general, the albedo of snow covered surfaces can be estimated using the following equation:

$$\alpha = 0.526\ (\rho[\text{TM2}]) + 0.232\ (\rho[\text{TM4}]) + 0.130\ (0.63\ (\rho[\text{TM4}])) + 0.112\ (\rho[\text{TM7}]). \quad (10)$$

However, when snow saturates in TM Bands 1, 2, and 3, TM Band 4 can be used to estimate reflectance for the 0.28- to 0.725-μm segment. Through the examination of typical snow reflectance curves (e.g., Dozier, 1984; Hall *et al.*, 1988), the reflectance of snow in TM Band 2 was evaluated as 1.12 times greater than that found in Band 4. Therefore, when saturation occurs in Bands 1, 2, and 3, the albedo of snow can be estimated as

$$\alpha = 0.526\ (1.12\ (\rho[\text{TM4}])) + 0.232\ (\rho[\text{TM4}]) + 0.130\ (0.63\ (\rho[\text{TM4}])) + 0.112\ (\rho[\text{TM7}]). \quad (11)$$

In this equation, TM Band 4 is used to represent the first part of the near-infrared region (0.725 to 1.00 μm). As in the visible portion of the spectrum, the selection of a representative band for the second portion of the near-infrared region (1.00 to 1.40 μm) presents an additional problem because no TM band falls in this region of the spectrum. Again, TM Band 4 is used to represent reflectance following the inspection of several spectral reflectance curves of snow. It was found that snow reflectance in the 1.00- to 1.40-μm spectral region is on average 0.63 times less than that of TM Band 4. Finally, TM Band 7 is employed to represent reflectance in the mid-infrared (1.40 to 6.00 μm).

TESTING OF THE MODEL

Description of the Study Area

A study area located in the Ward, Colorado 7.5-minute quadrangle was chosen for model testing (Figure 1). The area of Niwot Ridge was selected for comparison of model derived parameters with field measurements. Niwot Ridge is an east-west trending ridge extending a distance of some 10 km from Navajo Peak (4150 m) to Bald Mountain at 3530 m. Here, strong prevailing winds from the west control the distribution of snow cover. West facing slopes and ridge tops are generally free of snow, while east facing slopes usually accumulate a deep snowpack (Frank and Thorn, 1985). On Niwot Ridge, vegetation distribution is controlled by the complex relationships between topography, wind, insolation, and soil moisture. Mean annual temperature and precipitation are approximately −3.7°C and 1020 mm, respectively. The mean summer temperature is 7°C at an elevation of 3750 m, and winter snowfall averages 700 mm of water equivalent (Olyphant, 1986).

Data Used

The model described in this paper relies primarily on data collected by Landsat TM and DEMs. For this test, TM imagery was acquired under clear atmospheric conditions on 29 June 1984 at 10:12 AM. At this time period, the solar elevation angle is 60° and azimuth angle 116°. All six reflective TM bands from 0.45 μm to 2.35 μm were considered for reflectance calculations, but only three (TM2, TM4, and TM7) were used in the determination of surface albedo.

A 30-metre resolution DEM of Ward 7.5-minute quadrangle was acquired from the United States Geological Survey (USGS). In the study area, the elevation ranges from 2540 m to 4028 m. The DEM was used in the geometric correction of Landsat TM imagery, the calculation of shortwave irradiance, and the correction of atmospheric path radiance and transmittance in TM data. The DEM was particularly useful for deriving slope, aspect, angle of incidence, and shadows, all necessary for the removal of atmospheric and topographic effects. The Landsat TM image

was registered to the DEM by using a shaded relief image to identify ground control points (Duguay *et al.*, 1989).

Atmospheric temperature and humidity profiles collected from the nearby Denver station at 5:00 AM, on the date of Landsat-5 overpass, were used as inputs to the model for the computation of incoming solar radiation, atmospheric transmission, and path radiance over the study area. These radiosonde data were modified by interpolation to adjust the low altitude values to reflect the conditions occurring over the study area at 10:12 AM when the satellite passed overhead. This adjustment was necessary because inversions near the surface are frequent in early mornings at atmospheric levels near the ground.

Field observations consisted of surface albedo measurements obtained at several sites on Niwot Ridge during two field seasons (mid-June to mid-July, 1986 and 1987) at the time of day of Landsat-5 TM overflight (see Figure 1). Each site was selected on the basis of its accessibility and representativeness of the following surfaces: (1) dry alpine meadow (DM-1 and DM-2), (2) wet herbaceous meadow (WM), (3) snow (SF-1 and SF-2), and (4) scree (SC).

Computation of Model Parameters

Based on the radiosonde data and data on shortwave irradiance provided in Boer (1977) and NASA (1974), the two-stream model of Zdunkowski *et al.* (1982) was utilized to calculate the direct, diffuse sky, and total irradiance, and the path radiation and atmospheric transmission to unobstructed horizontal surfaces. The solar irradiance values found in Boer (1977) correspond to data for a cool summer day (clear, dry atmosphere) – conditions prevalent at the time of Landsat overflight for the study area. Computed irradiance values for horizontal surfaces at sea level and extraterrestrial irradiance for Landsat TM bands are presented in Table 2. As shown in this table, the contribution of diffuse sky irradiance to total irradiance in TM Bands 5 and 7 is null. As indicated by Iqbal (1983), diffuse sky irradiance at wavelengths greater than 1.00 μm is negligible.

Given estimates of all radiation fluxes for unobstructed horizontal surfaces, at heights defined by the levels of the radiosonde ascents, the DEM of the Ward 7.5-minute quadrangle was used to calculate values for direct, diffuse sky, and total irradiance, as well as path radiance and atmospheric transmission, for surfaces of varying elevation, slope, and aspect. Results of path radiance for the six reflective bands of TM, for two elevations found in the study area, are given in Table 3. Because diffuse irradiance is negligible in TM5 and TM7, corrections for path radiance were not deemed necessary for these bands.

Finally, once the irradiance and atmospheric parameters were determined, surface reflectance and albedo values were estimated, and an albedo map was produced. These results are discussed next.

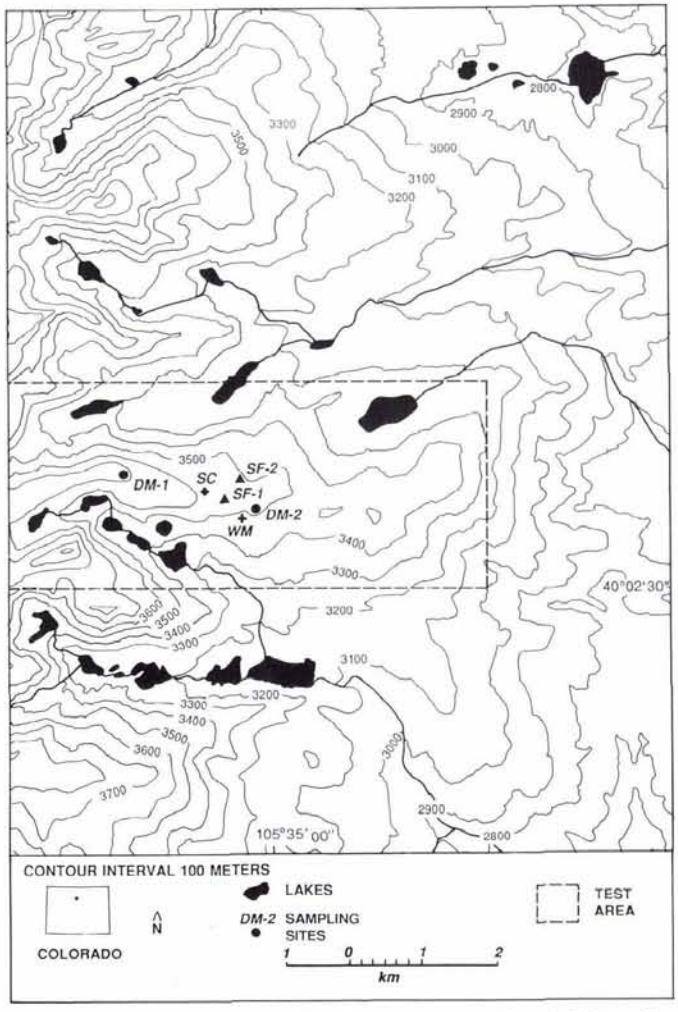

FIG. 1. Map of the study area (Ward 7.5-minute quadrangle). Sampling sites are identified as wet meadow (WM), dry meadow (DM-1 and DM-2), snow fields (SF-1 and SF-2), and scree (SC).

RESULTS

Comparison with Field Measurements and Literature

Surface reflectance

Landsat TM estimated surface in-band reflectance values of selected surfaces in the study area are presented in Table 4. The lack of concurrent field measurements of reflectance of the tundra of Niwot Ridge, snow fields, and the coniferous forest does not permit meaningful comparison between *in situ* and Landsat derived values at this stage. However, recent estimates of at-

TABLE 2. DIRECT, DIFFUSE SKY, AND TOTAL SOLAR IRRADIANCE AT SEA LEVEL ON A CLEAR-DRY SUMMER DAY AND EXOATMOSPHERIC SOLAR IRRADIANCE IN BANDWIDTHS COVERED BY LANDSAT-5 TM (29 JUNE 1984; LATITUDE 40°; SOLAR ELEVATION 60°) (IN Wm^{-2})

Band	Direct	Diffuse Sky	Total	Exoatmospheric Solar Irradiance
TM1	88.65	12.33	100.98	139.00
TM2	96.62	9.58	106.20	139.00
TM3	66.82	4.92	71.74	89.00
TM4	115.32	5.48	120.80	146.00
TM5	39.80	0.00	39.80	45.00
TM7	20.40	0.00	20.40	21.00

TABLE 3. RESULTS OF PATH RADIANCE* FOR TWO ELEVATIONS IN THE STUDY AREA CALCULATED FROM THE MODEL (29 JUNE 1984; SOLAR ELEVATION 60°; CLEAR-DRY ATMOSPHERE)

	Elevation (m)	
Band	2595	3965
TM1	2.04	1.74
TM2	1.58	1.35
TM3	0.81	0.69
TM4	0.91	0.77
TM5	---	---
TM7	---	---

*$Wm^{-2}sr^{-1}$

TABLE 4. ESTIMATED REFLECTANCE VALUES (MEAN AND STANDARD DEVIATION) FOR SELECTED SURFACES USING LANDSAT-5 TM BANDS

Surface	Band TM1	TM2	TM3	TM4	TM5	TM7
Coniferous Forest						
Mean	0.09	0.08	0.06	0.16	0.06	0.05
SD	0.01	0.01	0.01	0.01	0.01	0.01
n = 33						
Dry Meadow						
Mean	0.16	0.17	0.15	0.25	0.23	0.17
SD	0.01	0.01	0.01	0.01	0.01	0.01
n = 24						
Moist Meadow						
Mean	0.13	0.13	0.12	0.28	0.20	0.13
SD	0.01	0.01	0.01	0.02	0.02	0.02
n = 22						
Wet Meadow						
Mean	0.11	0.11	0.10	0.23	0.18	0.12
SD	0.01	0.01	0.01	0.01	0.01	0.01
n = 21						
Decaying Snow						
Mean	*	*	*	0.61	0.02	0.02
SD	*	*	*	0.01	0.01	0.01
n = 25						
Water						
Mean	0.09	0.08	0.06	0.07	0.02	0.03
SD	0.00	0.00	0.00	0.00	0.00	0.00
n = 25						

* Data saturation occurred n is the sample size

satellite (planetary) reflectance of snow by Dozier (1984) and Hall *et al.* (1988) enable some comparison with our data.

Reflectance measurements from TM Bands 4, 5, and 7 over snow indicate that this is a melting snowpack. The spectral reflectance values correspond to coarse old melting or refrozen snow. It has been shown that, in the visible, snow reflectance is less sensitive to grain size than in the near-infrared (Dozier, 1984). Saturation over snow in the visible (TM1, TM2, and TM3) was a problem, so estimates of snow reflectance were limited to the near-infrared (TM4) and mid-infrared (TM5 and TM7) bands.

Hall *et al.* (1988) measured the planetary reflectance of old snow on two glaciers (Austria and Alaska) under clear skies using Landsat TM imagery. They reported values of 0.62 and 0.63 for TM4, 0.03 and 0.01 for TM5, and 0.01 and 0.00 for TM7. Values in all three spectral bands are in good agreement with those derived over a melting snowpack on Niwot Ridge. Moreover, reflectance values in TM Bands 5 and 7 correspond well to those derived by Dozier (1984). Dozier reported reflectance values of 0.011 and 0.010 for TM5 and TM7, respectively, for a melting snowpack in the Sierra Nevada.

Surface albedo

Estimated and observed albedo values at several test sites over the alpine tundra of Niwot Ridge are given in Table 5. Derived albedo values for the coniferous forest to the northeast of Niwot Ridge, and lakes in the vicinity of the Ridge, can also be found. It can be seen from this table that estimated values of albedo for the surfaces found on Niwot Ridge, except for one of the two snowfields (i.e., SF-2), are in error by less than 0.02 from mean observed values.

The large discrepancy between observed and estimated albedo values at site SF-2 is conceivably related to differences in the state of the snowpack (contaminants, grain size, etc.) between the dates at which the data were recorded. At this site, the estimated values represent snow albedo in late June, 1984 while the observed values correspond to field measurements in late June, 1987. However, no marked differences are observable between observed and estimated values at SF-1 (1986 field season). Generally higher

TABLE 5. ESTIMATED ALBEDO VALUES FOR SELECTED SURFACES IN THE NIWOT RIDGE AREA

Surface (Test Site)	Estimated[1]	Observed
Decaying Snow		
(SF-1)	0.54/0.01/12	0.43
(SF-2)	0.55/0.02/13	0.56[2]
Dry Meadow		
(DM-1)	0.21/0.02/13	0.19
(DM-2)	0.20/0.01/15	0.19
Wet Meadow		
(WM)	0.15/0.00/13	0.16
Scree		
(SC)	0.23/0.01/12	0.22
Coniferous Forest	0.11/0.00/15	---
Water (Lakes)	0.08/0.00/12	---

[1]Format is mean / standard deviation / sample size
[2]Data collected during the 1986 field season

monthly total precipitation and lower temperatures recorded in the winter months (October to May) of the 1983-84 and 1985-86 periods at two climatological stations on Niwot Ridge provide a partial explanation for these differences.

Albedo values of melting snow covers have been reported by Aguado (1985) in a study site in the Sierra Nevada for three consecutive field seasons. Aguado found mean albedo values of 0.49, 0.45, and 0.48 for the 1981, 1982, and 1983 melt seasons, respectively. Similarly, LeDrew and Weller (1978) measured albedo values of 0.48 to 0.57 over a decaying snow bank on Niwot Ridge. Both sets of values reported by LeDrew and Weller (1978) and Aguado (1985) are within the range of estimated values and those observed during the 1986 field season on Niwot Ridge.

Surface albedo values for tundra vegetation, coniferous forests, and water have been reported by Sellers (1965), Barry and Chorley (1982), and Iqbal (1983). In these studies, we find albedo values for the tundra vegetation to vary between 0.11 and 0.23, those of coniferous forests from 0.05 to 0.15, and of water bodies in the 0.06 to 0.10 range. Again, estimated albedo values appear reasonable and are in substantial agreement with published data for comparable surfaces and measurements in the region.

EVALUATION OF THE ALBEDO MAP

Although estimated albedo values, for a limited number of test sites, are well within the range of albedo values reported in other studies, questions need to be answered regarding the quality of the produced albedo map. Sjoberg and Horn (1983) have proposed three subjective criteria for evaluating the quality of albedo maps so produced using remotely sensed imagery and digital terrain data. These criteria can be formulated in the form of questions. First, is there any visible evidence of terrain shape (effects due to changes in elevation, slope, and aspect) in the albedo map? Second, is the dynamic range of the set of computed albedo values reasonable; that is, do all values range from 0.00 to 1.00? Third, are the computed albedo values of sunlit and adjacent shadowed surfaces comparable, with no evidence of shadows? Another criterion which, we feel, also needs to be considered is the quality of DEMs – Is there any visible evidence of errors in derived albedo values due to the banding (or striping) effects observable in the shaded relief image of the study area?

The albedo map produced for Ward quadrangle (Plate 1a) does not seem to show any significant effect due to *terrain* shape or shadows, other than changes in ground cover. However, this is difficult to establish because in the study area variations in land-cover categories are generally controlled by changes in terrain height and aspect (Greenland *et al.*, 1985). One example

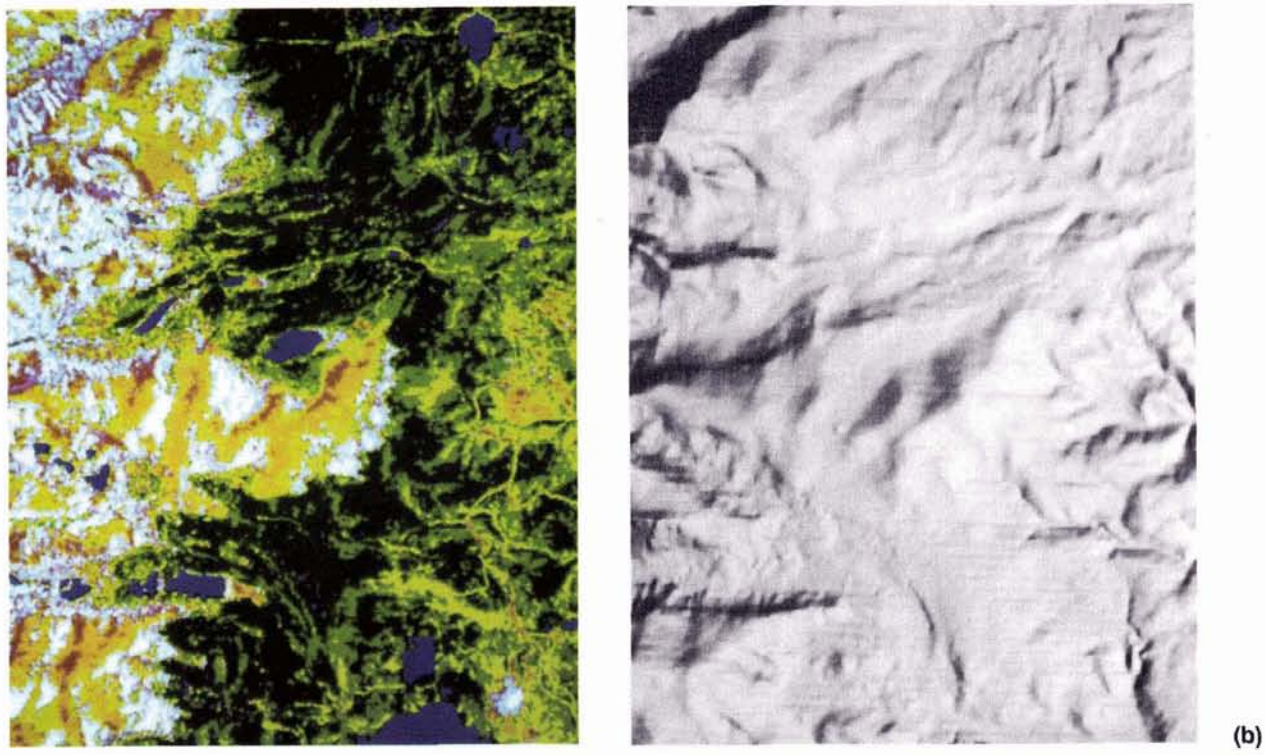

(a) (b)

PLATE 1. (a) Albedo map of Ward quadrangle. The albedo classes are the same as in Plate 2. (b) Shaded relief map of the Ward 7.5-minute quadrangle.

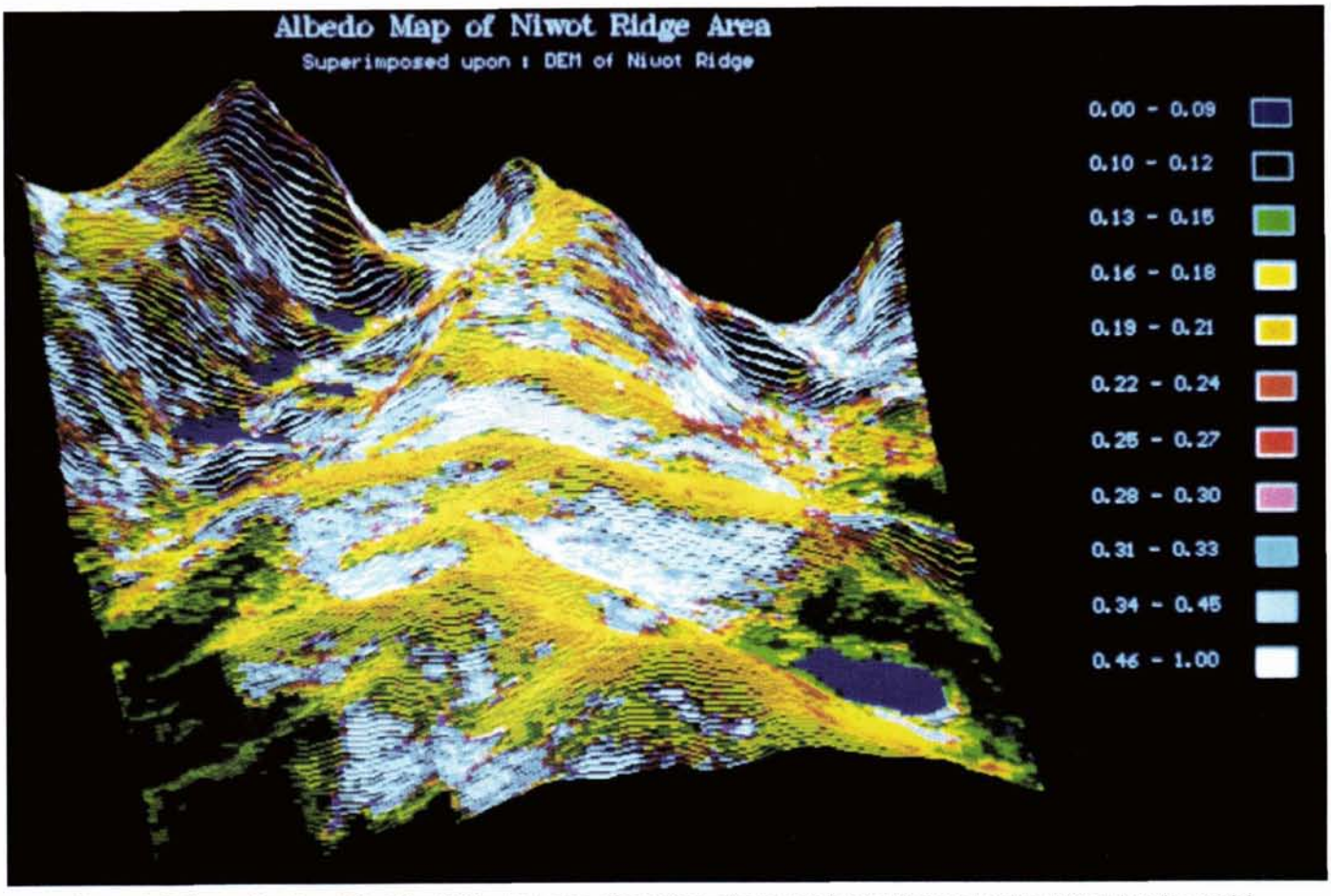

PLATE 2. Orthographic view of the Niwot Ridge test area. The surface albedo map is superimposed on the digital elevation model.

which shows the appropriateness of the proposed model in correcting for variable illumination effects is that of the northwest-facing and southeast-facing slopes bounding a valley in the northwest corner of the Ward quadrangle. With the range of albedo values found in this area, two different conclusions could be drawn. First, the correction procedure is inappropriate, thus resulting in higher albedo values on northwest-facing slopes than southeast-facing slopes. Second, changes in albedo values are related to changes in the nature of the surface material changes. The range of albedo values for snow covered areas found on both sides of the valley (0.54 to 0.56) suggest that the albedo differences are most likely to be due to changes in land-cover material. Effects due to path radiance and atmospheric transmission also seem to have been successfully removed, because the albedo of clear lakes and snow covered areas found at different elevation in the study area are within the same range of values.

The *dynamic range* of the set of computed albedo values has also been respected; that is, every calculated value in the study area lies between 0.00 and 1.00. The lowest albedo values were recorded for surfaces lying in cloud shadows and highest values for clouds. This is evident in the lower right corner of the Ward quadrangle (Plate 1a).

The *banding effect* which could be detected in the shaded relief map seems to have been filtered to some extent in the calculation process (Plates 1a and 1b). By examining the albedo map together with the shaded relief map, it can be seen that errors due to banding result in a maximum shift of one albedo class. This means that the worse case of banding in the DEM used in the present study could result in a maximum difference of 0.05 between albedo values calculated before and after corrections have been applied to the original DEM.

CONCLUSIONS

A model has been presented in order to estimate surface reflectance and albedo over rugged terrain. Using Landsat-5 TM imagery, digital terrain data, and radiosonde data, a two-stream radiative transfer scheme was applied successfully to derive reflectance and albedo for a range of surfaces, and to map the spatial distribution of surface albedo for a section of the east slope of the Colorado Front Range. Estimated values of albedo for selected surfaces in the alpine tundra zone were found to be in substantial agreement with published data for comparable surfaces and field measurements in the region.

Although the quality of most digital elevation data is currently being questionned (*e.g.*, Dozier, 1989), we have shown that reasonable estimates of surface albedo can be obtained. We do recommend, however, that care be taken when utilizing DEMs in simulation experiments, as well as in studies aimed at improving land-cover classifications of mountainous areas. Issues related to the quality of DEMs and possible propagation of errors in radiation modeling experiments should be examined further. In this paper, only a qualitative assessment of the quality of the albedo map was provided.

ACKNOWLEDGMENTS

This research was supported by an Natural Sciences and Engineering Research Council (NSERC) operating grant and WATDEC grant of computer equipment to E. LeDrew, and an NSERC operating grant to C. Duguay. The authors are grateful to the University of Colorado, Institute of Arctic and Alpine Research, Mountain Research Station for providing student scholarships to C. Duguay while a Ph.D. student at the University of Waterloo, and Dr. Christopher Brühl and Prof. Wilford Zdunkowski for provision of the radiative transfer code PIFM. The manuscript was greatly improved following the comments of three anonymous referees.

REFERENCES

Aguado, E., 1985. Radiation balances of melting snow covers at an open site in the central Sierra Nevada, California. *Water Resources Research*, 21(1):1649-1654.

Barry, R. G., and R. J. Chorley, 1982. *Atmosphere, Weather and Climate*. Methuen, London.

Boer, K. W., 1977. The solar spectrum at typical clear weather days. *Solar Energy*, 19:525-538.

Brest, C. L., 1987. Seasonal albedo of an urban/rural landscape from satellite observations. *Journal of Climate and Applied Meteorology*, 26(9):1169-1187.

Brest, C. L., and S. N. Goward, 1987. Deriving surface albedo measurements from narrow band satellite data. *International Journal of Remote Sensing*, 8(3):351-367.

Cavayas, F., G. Rochon, and P. Teillet, 1983. La mesure des réflectances bidirectionnelles par l'analyse des images Landsat. *Comptes rendus du 2e colloque international sur les signatures spectrales d'objets en télédétection*, Bordeaux, France, pp. 123-130.

Dozier, J., 1984. Snow reflectance from Landsat-4 Thematic Mapper. *IEEE Transactions on Geoscience and Remote Sensing*, GE-22(3):323-328.

———, 1985. Spectral signature of snow in visible and near-infrared wavelengths. *Proceedings of the Third International Colloquium on Spectral Signatures of Objects in Remote Sensing*, 16-20 December, Les Arcs, France, pp. 437-442.

———, 1989. Spectral signature of alpine snow cover from Landsat Thematic Mapper. *Remote Sensing of Environment*, 28:9-22.

Duguay, C., G. Holder, E. LeDrew, P. Howarth, and D. Dudycha, 1989. A software package for integrating digital elevation models into the digital analysis of remote sensing data. *Computers and Geosciences*, 15(5):669-678.

Frank, T. D., and C. E. Thorn, 1985. Stratifying alpine tundra for geomorphic studies using digitized aerial imagery. *Arctic and Alpine Research*, 17:179-188.

Greenland, D., J. Burbank, J. Key, L. Klinger, J. Moorhouse, S. Oaks and D. Shankman, 1985. The bioclimates of the Colorado Front Range. *Mountain Research and Development*, 5:221-239.

Hall, D. K., A. T. C. Chang, and H. Siddalingaiah, 1988. Reflectances of glaciers as calculated using Landsat-5 Thematic Mapper data, *Remote Sensing of Environment*, 25:311-321.

Hall, D. K., A. T. C. Chang, J. L. Foster, C. S. Benson, and W. M. Kovalick, 1989. Comparison of *in situ* and Landsat derived reflectance of Alaskan glaciers. *Remote Sensing of Environment*, 28:23-31.

Hay, J. E., 1983. Solar energy system design: the impact of the mesoscale variations in solar radiation. *Atmosphere-Ocean*, 21:138.

Iqbal, M., 1983. *An Introduction to Solar Radiation*. Academic Press, Toronto.

Kneizys, F. X., E. P. Shettle, L. W. Abreu, J. H. Chetwynd, Jr., G. P. Anderson, W. O. Gallery, J. E. A. Selby, and S. A. Clough, 1988. *Users Code to LOWTRAN 7*. AFGL-TR-88-0177 Environmental Research Papers, No. 1010, U.S. Department of Defense, Air Force Geophysics Laboratory, Optical Physics Division, 137 p.

LeDrew, E. F., and G. Weller, 1978. A comparison of the radiation and energy balance during the growing season for an arctic and alpine tundra. *Arctic and Alpine Research*, 10:665-678.

LeDrew, E., and C. Duguay, 1986. Radiation modelling in a high relief environment using a Landsat-5 TM image and DTM. *Proceedings of the Tenth Canadian Symposium on Remote Sensing*, 5-8 May, Edmonton, Alberta, pp. 559-564.

Liu, B. Y. H., and R. C. Jordan, 1960. The interrelationship and characteristic distribution of direct, diffuse and total solar radiation. *Solar Energy*, 4(3):1-19.

Malila, W. A., and D. M. Anderson, 1986. *Satellite Data Availability and Calibration Documentation for Land Surface Climatology Studies*. ISLSCP Report No. 5, 213 p.

National Aeronautics and Space Administration, 1974. *Surface Atmospheric Extremes: Launch and Transportation Areas*. NASA SP-8084 Technical Report, 77 p.

———, 1983. *Thematic Mapper Computer Compatible Tape (CCT-AT, CCT-PT)*. NASA Goddard Space-Flight Center, 184 p.

Olyphant, G. A., 1984. Insolation topoclimates and potential ablation in alpine snow accumulation basins: Front Range, Colorado. *Water Resources Research*, 20:491-498.

———, G. A., 1986. The components of incoming radiation within a mid-latitude alpine watershed during the snowmelt season. *Arctic and Alpine Research*, 18(2):163-169.

Proy, C., D. Tanré, and P. Y. Deschamps, 1989. Evaluation of topographic effects in remotely sensed data. *Remote Sensing of Environment*, 30:21-32.

Robinson, N., 1966. *Solar Radiation*. Elsevier, New York.

Sellers, W. D., 1965. *Physical Climatology*. University of Chicago Press, Chicago.

Sjoberg, R. W., and B. K. P. Horn, 1983. Atmospheric effects in satellite imaging of mountainous terrain. *Applied Optics*, 22:1702-1716.

Teillet, P. M., 1986. Image correction for radiometric effects in remote sensing. *International Journal of Remote Sensing*, 7(12):1637-1651.

Woodham, R. J., and T. K. Lee, 1985. Photogrammetric method for radiometric correction of Multispectral Scanner data. *Canadian Journal of Remote Sensing*, 11(2):132-161.

Woodham, R. J., and M. H. Gray, 1987. An analytic method for radiometric correction of satellite multispectral scanner data. *IEEE Transactions on Geoscience and Remote Sensing*, GE-25(3):258-271.

Yang, C., and A. Vidal, 1990. Combination of digital elevation models with SPOT-1 HRV multispectral imagery for reflectance factor mapping. *Remote Sensing of Environment*, 32:35-45.

Zdunkowski, W. G., W. -G. Panhans, R. M. Welch, and G. J. Korb, 1982. A radiation scheme for circulation and climate models. *Beiträge zur Physik der Atmosphäre*, 55:215-238.

(Received 10 September 1990; revised and accepted 21 August 1991)